DALTON PERSPECTIVE

Non-innocent behaviour in mononuclear and polynuclear complexes: consequences for redox and electronic spectroscopic properties

Michael D. Ward * and Jon A. McCleverty

School of Chemistry, University of Bristol, Cantock's Close, Bristol, UK BS8 1TS.
E-mail: mike.ward@bristol.ac.uk

Received 6th November 2001, Accepted 13th December 2001
First published as an Advance Article on the web 10th January 2002

This article reviews recent work in the area of non-innocent behaviour in polynuclear metal complexes. Non-innocence, which occurs when metal-based and ligand-based redox orbitals are similar in energy, has been known since the first dithiolene complexes of the Ni triad. Our recent work in this field is with complexes of two distinct types: polynuclear complexes of Ru(II) with dioxolene-type bridging ligands; and dinuclear complexes based on tris-(pyrazolyl)borato-Mo(V) or -Mo(I) units linked by bis-phenolate or bis-pyridyl bridging ligands. Detailed redox and UV/Vis/NIR spectroelectrochemical studies on these complexes have been carried out. An important point which emerges is that non-innocent behaviour in dinuclear complexes is an essential prerequisite for strong metal–metal electronic coupling across extended bridging ligands. Many of the complexes studied show intense charge-transfer transitions in the near-IR region of the spectrum, and the use of these in prototypical optical devices is briefly discussed.

1. Introduction

Complexes of non-innocent ligands have been of special interest in coordination chemistry since the preparation and study of the planar dithiolene complexes of nickel, palladium and platinum nearly 40 years ago.[1] In these complexes—and many related ones—the ambiguity in assignment of oxidation states to metal and ligand (Fig. 1), and the consequent confusion concerning the interpretation of the redox and electronic spectroscopic properties of the complexes, resulted in a debate on their exact nature which has lasted for many years. Since these dithiolene complexes were first studied, many other examples of

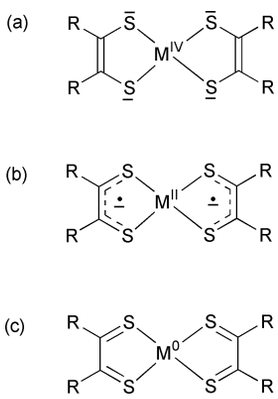

Fig. 1 Three possible resonance descriptions for the planar bis-dithiolene complexes with M = Ni, Pd, Pt. In the intermediate form (b), the two radical monoanions must be antiferromagnetically coupled.

Mike Ward was born in 1964. After a B.A. and Ph.D. from Cambridge, where he worked with Professor Ed Constable, he did post-doctoral work in the group of Professor Jean-Pierre Sauvage in Strasbourg before joining the School of Chemistry in Bristol as a new lecturer in 1990. His research interests cover all aspects of coordination chemistry, in particular the syntheses of polynuclear complexes, by either traditional or self-assembly methods, and the study of their physical properties (electrochemical, magnetic, optical, and photophysical). He was awarded the Royal Society of Chemistry's Corday Morgan medal for 1999, and the Sir Edward Frankland fellowship for 2000–2001, and is now a Professor of Inorganic Chemistry at Bristol.

Jon A. McCleverty **Michael D. Ward**

Jon McCleverty was born in 1937. After a Ph.D. with Sir Geoffrey Wilkinson at Imperial College and post-doctoral work with Professor Al Cotton at MIT, he joined the Chemistry department at Sheffield as a new lecturer in 1964. He moved to the University of Birmingham to take the first Chair of Inorganic Chemistry in 1980, and then moved to the Chair of Inorganic Chemistry at the University of Bristol in 1990 following the retirement of Professor Gordon Stone. His research interests cover many areas of coordination and materials chemistry including the chemistry of metal nitrosyl complexes; development of new tris(pyrazol-1-yl)borate ligands, and the synthesis of new metal complexes for non-linear optics. The most recent of numerous honours for his research is the current Royal Society of Chemistry Ronald Nyholm lectureship. He has been heavily involved with the EPSRC and the Royal Society of Chemistry at many levels, being currently chairman of the Scientific Affairs Board of the RSC.He represents chemistry on behalf of both the RSC and the EPSRC in various European and other international organisations.

DOI: 10.1039/b110131p

complexes displaying non-innocent behaviour have been found. Amongst the most well-known are complexes of the redox-active 1,2-dioxolene ligands (the catecholate/semiquinone/quinone series; Fig. 2, X = Y = O), which have

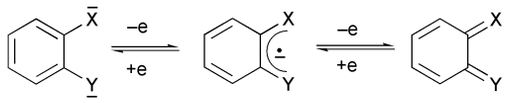

$(cat)^{2-}$ $(sq)^{-}$ q

Fig. 2 The dioxolene redox series (X = Y = O) catecholate (cat), semiquinonate (sq) and quinone (q). Strictly speaking these names only apply to the derivatives with X = Y = O (*e.g.* catechol is 1,2-dihydroxybenzene only), but the same labels are also commonly used for related ligands (*e.g.* X = Y = NH; X = O, Y = NH; X = S, Y = NH *etc.*) to emphasise the similarity in their oxidation state description.

been extensively studied by the groups of Pierpont[2,3] and Lever;[4,5] and their structural analogues with other donor atoms (Fig. 2, X, Y = NH, S).[6,7] For example Wieghardt and co-workers have recently studied in depth the non-innocent behaviour of structurally related ligands such as *o*-imino-benzosemiquinone derivatives, which are N,O-donor analogues of 'conventional' *o*-semiquinones, and have shown that ligands previously thought to be innocent can in fact be redox active in their complexes.[7] It is notable that all of these ligands have the same fundamental structural type as the dithiolenes, which provided the initial inspiration for their study, in that they are bidentate chelates based on a 1,2-disubstituted phenyl ring.

It is worth asking at this point exactly what is meant by the term 'non-innocent'. Jørgensen pointed out in 1966 that "ligands are innocent when they allow oxidation states of the central atoms to be defined", a definition which subtly emphasises that non-innocent behaviour depends on the metal as well as the ligand.[8] However the term 'non-innocent' is often (inaccurately) taken to mean simply that the ligands in a complex are redox-active, such that non-innocence is a function of the ligand alone—hence the common expression 'non-innocent ligands' in relation to *e.g.* dithiolenes and dioxolenes. This is not helpful in complexes where the metal-centred and ligand-centred frontier orbitals are at very different energies such that their redox potentials are widely separated. For example $[Ru(bpy)_3]^{2+}$ (bpy = 2,2′-bipyridine) undergoes metal-centred oxidation at +1.26 V *vs.* NHE and a series of ligand-centred reductions starting at −1.35 V; these redox processes can be assigned as metal- or ligand-centred without any ambiguity because of the substantial energy difference between the metal d(π) HOMO and the ligand π* LUMO orbitals where the redox processes take place.[9] In contrast, $[Cr(bpy)_3]^{3+}$ displays a series of one-electron reductions[10] whose assignment is more difficult because metal- and ligand-centred redox orbitals are comparable in energy.[11] Whereas the first reduction is metal-centred to give $[Cr^{II}(bpy)_3]^{2+}$, the next reduction results in transfer of (approximately) *two* electrons to the ligand π* levels to give a species best described as $[Cr^{III}(bpy)(bpy^{\bullet-})_2]^{+}$, and further reductions also result in 'delocalised' behaviour.[11,12] Thus the ligand bpy is redox active in both $[Ru(bpy)_3]^{2+}$ and $[Cr(bpy)_3]^{2+}$, but the description 'non-innocent' applies far more to the latter complex than the former. Likewise, the difficulty with the dithiolene complexes in Scheme 1 is not just that the ligands are redox active, but that there is strong mixing between ligand and metal frontier orbitals, such that assignment of oxidation states to individual metal and ligand components is difficult. In some cases, ligand- and metal-centred redox orbitals can be so close that the complexes display 'redox isomerism'; for example Pierpont has described a cobalt-dioxolene complex which switches between Co^{II}(sq) and Co^{III}(cat) forms as a function of temperature.[4] The term 'non-innocent' therefore is more appropriately applied to particular *combinations* of metal and ligand rather than to redox-active ligands alone, which is implicit in Jørgensen's original definition.

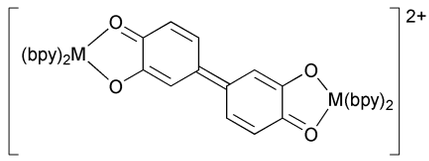

$[\mathbf{1\text{-}Ru}]^{2+}$ (M = Ru)
$[\mathbf{1\text{-}Os}]^{2+}$ (M = Os)

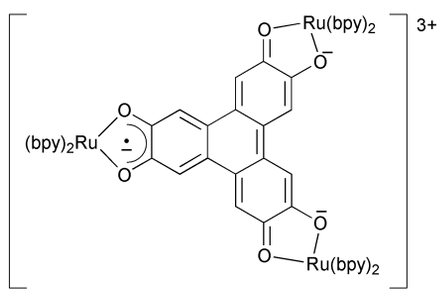

$[\mathbf{2\text{-}Ru}]^{3+}$

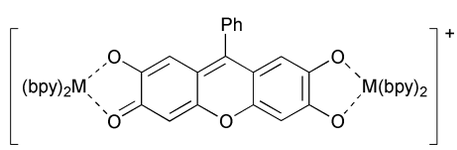

$[\mathbf{3\text{-}Ru}]^{+}$ (M = Ru)
$[\mathbf{3\text{-}Os}]^{+}$ (M = Os)

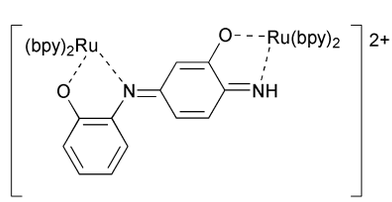

$[\mathbf{4\text{-}Ru}]^{2+}$

Scheme 1

This Perspective article reviews our recent work on the electrochemical and spectroscopic properties of complexes displaying non-innocent behaviour. The two major types of complex studied are (i) complexes of Ru(II) and Os(II) co-ordinated to dioxolene-type ligands (and their nitrogen-donor analogues); and (ii) complexes containing two tris(pyrazolyl)-borato-molybdenum units attached to either end of bis(pyridyl) or bis(phenolate) bridging ligands. The two apparently quite different sets of complexes have many fundamental similarities arising from their non-innocent behaviour, such as in the way that metal–metal electronic interactions vary across different bridging ligands, and in the appearance of intense, low-energy charge-transfer transitions in their electronic spectra which are redox-switchable and which make the complexes of interest as potential electrochromic dyes.

2. Polynuclear ruthenium and osmium complexes with bridging ligands having multiple dioxolene binding sites

(a) Introduction

In 1986, Lever *et al.* described the properties of the complex $[Ru^{II}(bpy)_2(cat)]$ (where H_2cat = catechol).[5] This complex

undergoes two reversible one-electron oxidations, to give species which were formulated on the basis of spectroscopic, structural and theoretical studies as $[Ru^{II}(bpy)_2(sq)]^+$ and $[Ru^{II}(bpy)_2(q)]^{2+}$, although this is not completely clear-cut with EPR and crystallographic studies showing that $[Ru^{II}(bpy)_2(sq)]^+$ does have some $[Ru^{III}(bpy)_2(cat)]^+$ character. The two oxidations are therefore largely ligand-centred, with the metal centre remaining formally in oxidation state +2 throughout the redox series, although there is strong mixing between metal and ligand frontier orbitals [oxidation of the metal centre to Ru(III) requires a very high positive potential and is irreversible]. A notable feature of these complexes is the presence of intense charge-transfer transitions. In $[Ru^{II}(bpy)_2(sq)]^+$ the HOMO–LUMO transition is $Ru^{II}[d(\pi)] \longrightarrow$ sq(SOMO) metal-to-ligand charge-transfer at 890 nm; in $[Ru^{II}(bpy)_2(q)]^{2+}$ the $Ru^{II}[d(\pi)] \longrightarrow q(\pi^*)$ MLCT transition is at higher energy, *viz.* 640 nm ($\varepsilon \approx 10^4$ M^{-1} cm^{-1} in each case). A few years later Pierpont *et al.* prepared the osmium analogue $[Os^{II}(bpy)_2(cat)]$.[13] This also undergoes two reversible one-electron oxidations, at potentials similar to those of $[Ru^{II}(bpy)_2(cat)]$, but in this case structural and EPR spectroscopic studies showed that the first oxidation is metal-centred, giving $[Os^{III}(bpy)_2(cat)]^+$, in agreement with the expected greater ease of oxidation of the third-row metal ion. The nature of the doubly oxidised form was not clear: the two limiting possibilities are $[Os^{IV}(bpy)_2(cat)]^{2+}$, following a second metal-based oxidation, or $[Os^{III}(bpy)_2(sq)]^{2+}$, following ligand-based oxidation.

(b) Ru complexes with poly-dioxolene ligands

We reasoned that preparation of bridging ligands containing several chelating dioxolene sites linked together, such that there is a conjugated connection between them, would result in polynuclear complexes containing very rich redox and spectroscopic behaviour, and so it proved. Complex **1-Ru** is effectively a dimer of $[Ru^{II}(bpy)_2(cat)]$ in which the two dioxolene units are linked 'back-to-back' (Scheme 1).[14] Given that $[Ru^{II}(bpy)_2(cat)]$ displays two ligand-centred redox processes linking three oxidation levels,[5] we expected **1** to display four ligand-centred redox processes linking five oxidation levels, from the fully reduced bis-catecholate form to the fully oxidised bis-quinone form (Fig. 3). The separation of 320 mV between the two cat/sq couples arises from the electrostatic interaction between two ligand-centred redox processes that are spatially close together. That the separation between the two sq/q couples is very similar (340 mV) indicates that the two sq/q couples interact to the same extent as do the two cat/sq couples, because they are also dioxolene-centred and the electrons involved are therefore about the same distance apart. All four redox processes are therefore ligand centred, a fact which is of particular significance when compared with the behaviour of the analogous osmium complex (see later).

An interesting feature of the behaviour of this complex is that the 'bis-semiquinone' (sq–sq) form $[\mathbf{1\text{-}Ru}]^{2+}$—in which the complex is actually isolated under aerobic conditions—is diamagnetic with a double bond between the phenyl rings. If the bridging ligand is drawn such that each dioxolene terminus has a normal semiquinone structure (*cf.* Fig. 2) with an unpaired electron, it is immediately apparent that the linkage between them allows the two electrons to pair up, resulting in a planar, extensively delocalised bridging ligand. The effect of this on the electronic spectrum of the complex is dramatic: the Ru(II) $\longrightarrow$ (sq–sq) MLCT transition is at lower energy (1080 nm) and much more intense (ε = 37,000 M^{-1} cm^{-1}) than in the mononuclear complex (Fig. 4).[14]

A UV/Vis/NIR spectroelectrochemical study using an OTTLE (Optically Transparent Thin-Layer Electrode) cell showed that this strong NIR absorption disappears in the fully reduced (cat–cat) form of the complex, consistent with the behaviour of the mononuclear $[Ru(bpy)_2(sq)]^+/[Ru(bpy)_2(cat)]$ couple, and that it shifts to higher energy (750 nm) in the fully oxidised (q–q) form, consistent with the behaviour of the mononuclear $[Ru(bpy)_2(sq)]^+/[Ru(bpy)_2(q)]^{2+}$ couple.[5] In the mixed-valence forms $[\mathbf{1\text{-}Ru}]^+$ (sq–cat) and $[\mathbf{1\text{-}Ru}]^{3+}$ (sq–q) the electronic spectra show delocalised behaviour, with (for example) a single Ru $\longrightarrow$ (bridging ligand) MLCT for $[\mathbf{1\text{-}Ru}]^{3+}$ rather than distinct Ru(II) $\longrightarrow$ sq and Ru(II) $\longrightarrow$ q transitions associated with valence-trapped termini. The behaviour of this complex has obvious similarities to that of the redox series $[\mathbf{RuN_4Ru}]^{n+}$ described by Lever, based on the analogous N-donor bridging ligand 3,4,3′,4′-tetraimino-biphenyl (Fig. 5),[15] although the redox potentials for the series $[\mathbf{1\text{-}Ru}]^{n+}$ are all more

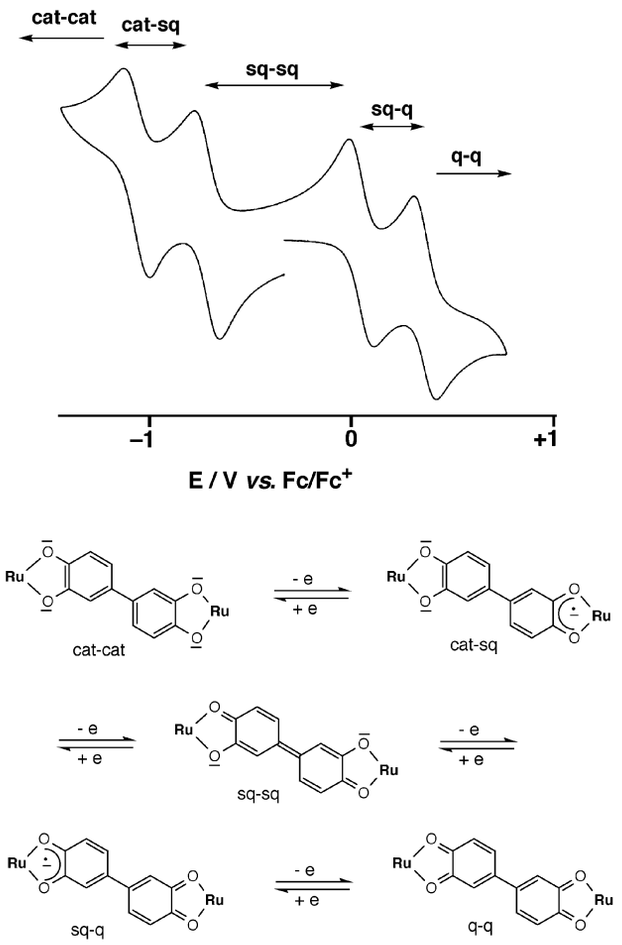

Fig. 3 The five-membered redox chain of $[\mathbf{1\text{-}Ru}]^{n+}$ (n = 0–4); the complex is isolated in the n = +2 state in aerobic conditions.

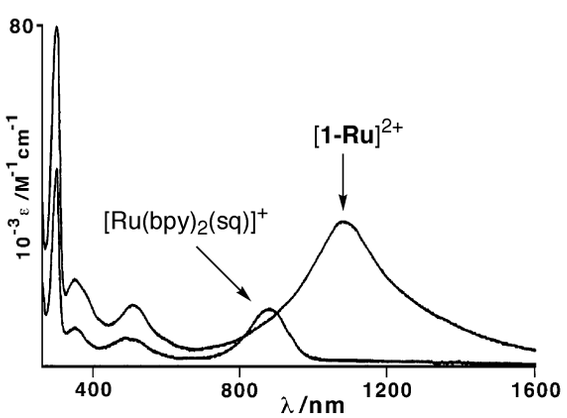

Fig. 4 Comparison of the lowest energy Ru $\longrightarrow$ dioxolene MLCT transitions of mononuclear $[Ru(bpy)_2(sq)]^+$ and dinuclear $[\mathbf{1\text{-}Ru}]^{2+}$ (in the sq–sq state).

positive than the corresponding processes of $[\mathbf{RuN_4Ru}]^{n+}$ and are all fully chemically reversible.

The spectroscopic behaviour of the redox series $[\mathbf{1\text{-}Ru}]^{n+}$ illustrates a common feature of many of the complexes described in this article (not to mention many other complexes displaying non-innocent behaviour). The fact that metal and ligand frontier orbitals are close in energy means that low-energy charge-transfer transitions are inevitable, which are fully allowed and therefore intense. This behaviour is not just an academic curiosity; the near-IR region of the electromagnetic spectrum (*ca.* 800–2000 nm) is of technological interest for several reasons. Transmission of optical signals down silica fibre-optic cables, which is of importance for telecommunications, uses near-IR light in the 1300–1500 nm region, where silica is transparent and will not attenuate the signal. Redox-active complexes which display a strong absorbance in this region of the spectrum in some oxidation states but not in others are accordingly of interest as switchable electrochromic dyes which could be used to modulate optical signals (electro-optic switching).[16] They could also be used in 'smart windows' which filter out radiant heat (*i.e.* near IR radiation) whilst transmitting visible light.[16] In addition, dyes used as sensitisers in solar cells ideally need to have an absorption spectrum matching the solar emission spectrum, which extends into the near-IR region.[17] An interesting spin-off of our fundamental studies on non-innocent polynuclear complexes has been the investigation of such complexes for applications of this sort.

Complex $[\mathbf{2\text{-}Ru}]^{3+}$ is prepared from the bridging ligand hexahydroxytriphenylene, and contains three dioxolene-like binding sites linked in a conjugated triangular array (Scheme 1).[18] In aerobic conditions this complex is isolated in the form in which each dioxolene site is in the semiquinone oxidation level (denoted sq–sq–sq) as shown in Scheme 1. If the ligand is drawn such that there is an unpaired electron associated with each of the semiquinone sites, any two can pair up (*cf.* the behaviour of $[\mathbf{1Ru}]^{2+}$ which is diamagnetic in its sq–sq oxidation state) to give a mono-radical in which the unpaired electron is delocalised over all three sites. If each dioxolene site shows the normal redox activity, we now expect six redox processes linking a seven-membered redox chain in which the bridging ligand changes from cat–cat–cat (fully reduced) to q–q–q (fully oxidised) forms. Voltammetric experiments did

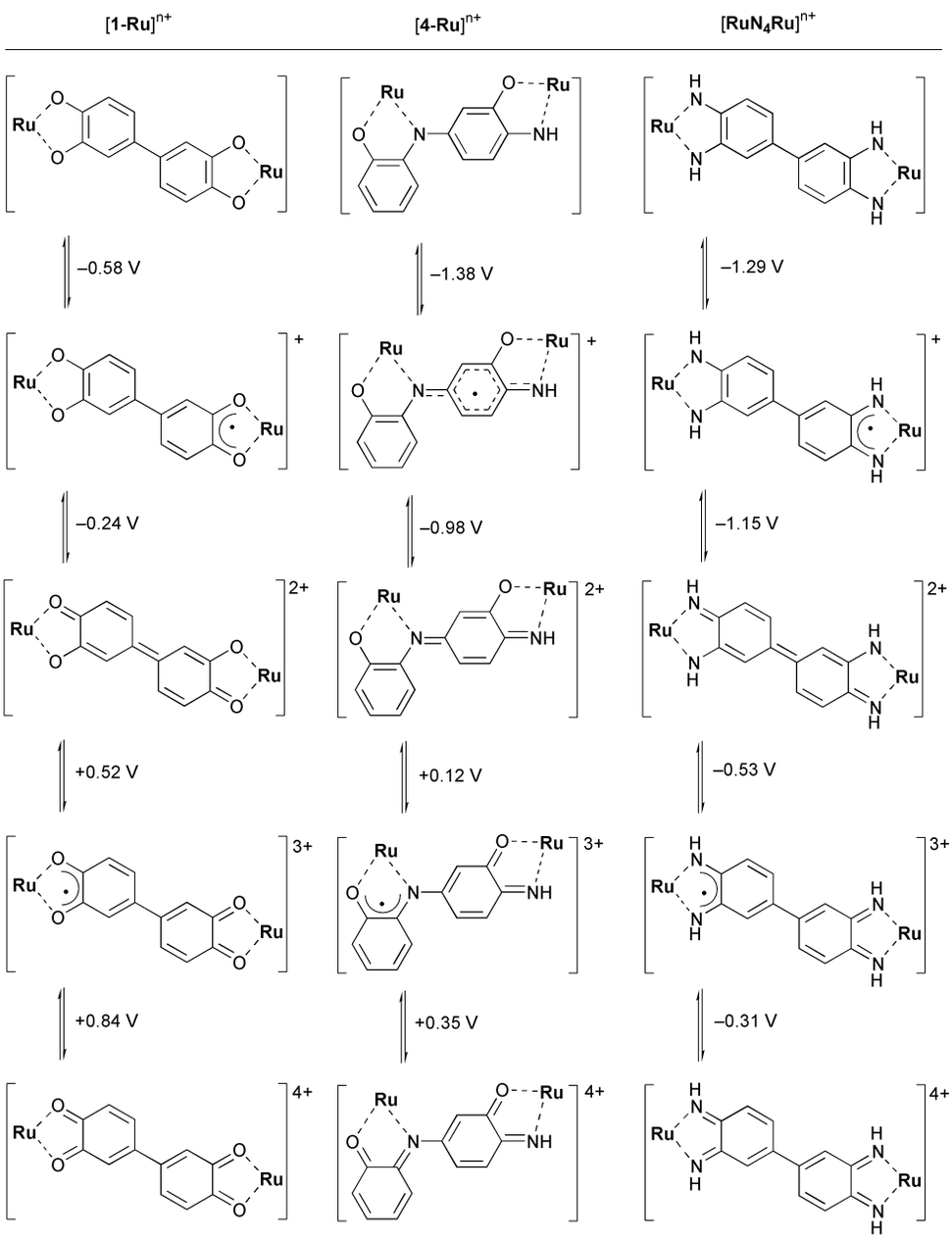

Fig. 5 Comparison of the five-membered redox chains of the complexes $[\mathbf{1\text{-}Ru}]^{n+}$, $[\mathbf{4\text{-}Ru}]^{n+}$ and $[\mathbf{RuN_4Ru}]^{n+}$ ($n = 0$, cat–cat state; $n = 1$, cat–sq; $n = 2$, sq–sq; $n = 3$, sq–q; $n = 4$, q–q). The data for the $[\mathbf{RuN_4Ru}]^{n+}$ series are taken from ref. 15 by Auburn and Lever; all potentials are *vs.* SCE.

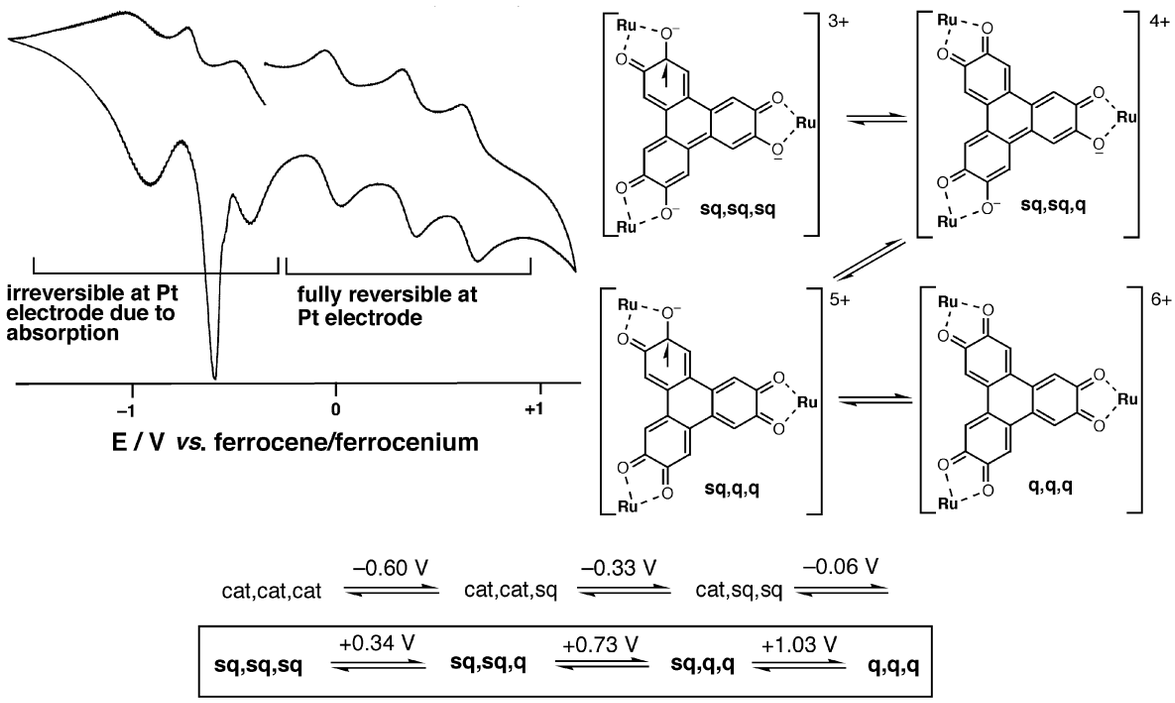

Fig. 6 The seven-membered redox chain of $[\mathbf{2\text{-}Ru}]^{n+}$ ($n = 0$–6); only the three most positive redox processes [from the $n = +3$ (sq–sq–sq) to the $n = +6$ (q–q–q) states] are fully reversible at a Pt electrode; the redox potentials in the scheme are *vs.* SCE.

indeed reveal the presence of six redox processes, but only the three most positive of these are chemically reversible, such that the complex can be interconverted between $[\mathbf{2\text{-}Ru}]^{3+}$ (sq–sq–sq) and $[\mathbf{2\text{-}Ru}]^{6+}$ (q–q–q) states and the two states in between, but reduction to $[\mathbf{2\text{-}Ru}]^{2+}$ (sq–sq–cat) or more reduced states results in deposition on the electrode and/or decomposition (Fig. 6).

The complex $[\mathbf{2\text{-}Ru}]^{3+}$ shows a very intense, low-energy MLCT transition ($\lambda_{max} = 1170$ nm, $\varepsilon = 40{,}000$ M^{-1} cm^{-1}).[18] This is analogous to the Ru(II) ⟶ sq MLCT transitions of mononuclear $[Ru(bpy)_2(sq)]^+$ (890 nm) and dinuclear $[\mathbf{1\text{-}Ru}]^{2+}$ (1080 nm), but this time involving the more extensively delocalised SOMO of the bridging ligand in its sq–sq–sq state, which is reflected in the lower energy of the transition. UV/Vis/NIR spectroelectrochemistry (Fig. 7) showed how as the complex is oxidised in steps to $[\mathbf{2\text{-}Ru}]^{4+}$ (sq–sq–q), $[\mathbf{2\text{-}Ru}]^{5+}$ (sq–q–q) and finally $[\mathbf{2\text{-}Ru}]^{6+}$ (q–q–q), the MLCT transition is blue-shifted in steps from 1170 nm to 759 nm. The 'mixed valence' sq–sq–q and sq–q–q states are therefore delocalised (*cf.* the behaviour of $[\mathbf{1\text{-}Ru}]^{3+}$ in the sq–q state) because a single MLCT transition at a weighted average position occurs, rather than distinct transitions involving localised sq and q sites of the bridging ligand.

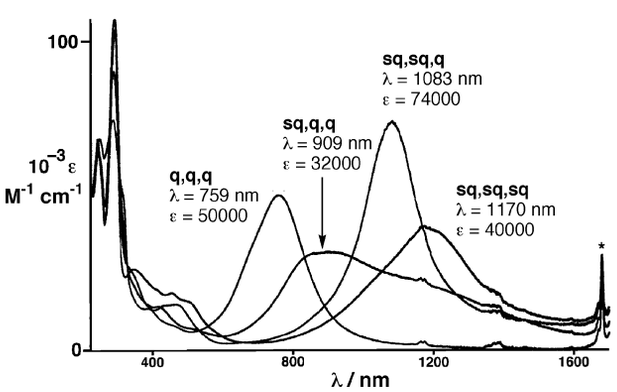

Fig. 7 UV/Vis/NIR spectroelectrochemical study of $[\mathbf{2\text{-}Ru}]^{n+}$ (n = 3–6) in MeCN, showing how the principal Ru ⟶ (bridging ligand) MLCT transition is blue-shifted as the bridging ligand is oxidised. (The * denotes a solvent vibrational overtone band).

Assignment of redox processes as metal- or ligand-centred is more difficult in complex $[\mathbf{3\text{-}Ru}]^+$ which is based on the commercially available bridging ligand 9-phenyl-2,3,7-trihydroxyfluorone.[19] In this complex the diamagnetic bridging ligand may be considered as formally in the cat–sq oxidation level, with one dianionic catecholate-like terminus and one monoanionic semiquinone-like terminus, although its closed-shell nature means that it cannot act as an electron-acceptor for MLCT transitions until it is oxidised (in this respect the fully reduced form of the bridging ligand is analogous to a catecholate). In fact delocalisation renders the two termini equivalent, as was apparent from the ^{1}H NMR spectrum. Compared to the redox series $[\mathbf{1\text{-}Ru}]^{n+}$ and $[\mathbf{2\text{-}Ru}]^{n+}$ described above, it is less obvious in this case how many ligand-centred redox processes are expected: we might expect at least two oxidations of the 'cat' terminus to a 'q' unit, giving a 'sq–q' state, but it is not possible to draw sensible valence structures for ligand states more reduced than cat–sq or states more oxidised than sq–q. In fact $[\mathbf{3\text{-}Ru}]^+$ shows three reversible redox processes, at −0.36, 0.00 and +0.53 V *vs.* Fc/Fc^+ (Fig. 8) so it sensible to assign at least one as ligand-based. The results of the UV/Vis/NIR spectroelectrochemical study spanning the four oxidation states $[\mathbf{3\text{-}Ru}]^+$ to $[\mathbf{3\text{-}Ru}]^{4+}$ (Fig. 8) are comparable to those for $[\mathbf{2\text{-}Ru}]^{n+}$ (n = 3–6), with intense absorptions in the near-IR region which are strongly electrochromic, although their assignment here is tentative. A ZINDO calculation on the diamagnetic oxidation state $[\mathbf{3\text{-}Ru}]^+$ showed that the HOMO is strongly delocalised between metal ions and bridging ligand, with the lowest-energy absorption manifold at 714 nm containing a mixture of Ru ⟶ bpy MLCT and cat ⟶ bpy LLCT transitions. As the oxidations proceed it is expected that Ru ⟶ (bridging ligand) MLCT transitions will occur as holes appear in the bridging ligand HOMO and this appears to be the case with, for example, a transition at 1237 nm (ε = 41,000 M^{-1} cm^{-1}) appearing for $[\mathbf{3\text{-}Ru}]^{3+}$.

(c) Os complexes with poly-dioxolene ligands

The osmium analogues of the above Ru complexes were also studied, and comparison of the redox properties of $[\mathbf{1\text{-}Os}]^{n+}$, $[\mathbf{2\text{-}Os}]^{n+}$ and $[\mathbf{3\text{-}Os}]^{n+}$ with those of $[\mathbf{1\text{-}Ru}]^{n+}$, $[\mathbf{2\text{-}Ru}]^{n+}$ and $[\mathbf{3\text{-}Ru}]^{n+}$

proved particularly informative (Fig. 9).[20] The cyclic voltammogram of $[\mathbf{1\text{-}Os}]^{n+}$ (n = 0–4) shows four redox processes linking a chain of five oxidation states, exactly as does $[\mathbf{1\text{-}Ru}]^{n+}$. However, the first two couples (at negative potential) are much closer together ($\Delta E_{1/2}$ = 100 mV) than in $[\mathbf{1\text{-}Ru}]^{n+}$ ($\Delta E_{1/2}$ = 320 mV), whereas the second two processes are separated by almost exactly the same amount (330 *vs.* 340 mV). This implies that in $[\mathbf{1\text{-}Os}]^{n+}$, the first two redox couples are metal-centred Os(II)/Os(III) couples which are weakly interacting because they are spatially remote, but the second two redox couples are ligand-centred and therefore closer together and more strongly interacting. Whereas $[\mathbf{1\text{-}Ru}]^{2+}$ is best described as Ru^{II}(sq–sq)-Ru^{II}, $[\mathbf{1\text{-}Os}]^{2+}$ is best described as Os^{III}(cat–cat)Os^{III}, in agreement with the relative behaviour of the mononuclear complexes $[Ru^{II}(bpy)_2(sq)]^+$ and $[Os^{III}(bpy)_2(cat)]^+$. Further, the fact that the two more positive redox couples are ligand-centred means that $[\mathbf{1\text{-}Os}]^{4+}$ is best described as Os^{III}(sq–sq)Os^{III}, in contrast to

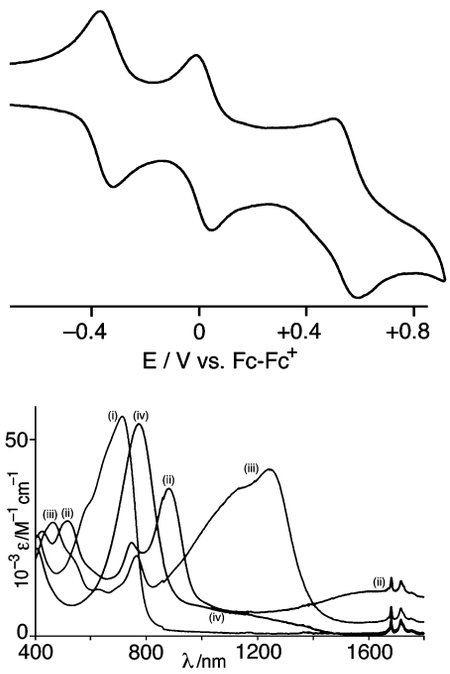

Fig. 8 Cyclic voltammogram (top) and UV/Vis/NIR spectroelectrochemistry (bottom) of $[\mathbf{3\text{-}Ru}]^{n+}$ (n = 1–4) in MeCN (i, n = 1; ii, n = 2; iii, n = 3; iv, n = 4).

Ru^{II}(q–q)Ru^{II} for $[\mathbf{1\text{-}Ru}]^{4+}$. This provides indirect evidence that the two oxidations of $[Os^{II}(bpy)_2(cat)]$ are successively metal and then ligand-centred to give $[Os^{III}(bpy)_2(sq)]^{2+}$, which rules out the alternative possibility of $[Os^{IV}(bpy)_2(cat)]^{2+}$ for the doubly-oxidised form.[13]

Exactly similar behaviour was shown by $[\mathbf{3\text{-}Os}]^+$;[20] comparison of its CV with that of $[\mathbf{3\text{-}Ru}]^+$ shows that the separation between the first two redox couples has dropped from 360 mV in $[\mathbf{3\text{-}Ru}]^+$ to 150 mV in $[\mathbf{3\text{-}Os}]^+$, but the third process at a more positive potential has changed very little. This is again consistent with the first two redox processes being metal-localised Os(II)/Os(III) couples and being spatially remote from one another, rather than having substantial ligand-centred character (and being closer together) as was the case for $[\mathbf{3\text{-}Ru}]^+$. For $[\mathbf{3\text{-}Os}]^+$ we can accordingly assign the first two oxidations as metal-based and the third as centred on the bridging ligand. This knowledge helped in assigning the electronic spectra of the different oxidation states, although this is offset by the much greater spin–orbit coupling of Os which results in transitions that were spin-forbidden for Ru becoming apparent and complicating the assignments.

For the trinuclear complex $[\mathbf{2\text{-}Os}]^{3+}$, following the above arguments the formulation $(Os^{III})_3$(cat–cat–cat) is expected, in contrast to $(Ru^{II})_3$(sq–sq–sq). We would expect therefore to see three metal-centred $Os^{III} \longrightarrow Os^{II}$ reductions which are close together, and three ligand-centred cat $\longrightarrow$ sq oxidations which are well separated. Unfortunately in the CV the reductions are obscured by surface absorption processes to the extent that it is not even possible to see how many there are; however, the three ligand-centred oxidations are well-separated (*ca.* 300 mV between successive couples), exactly as they are in $[\mathbf{2Ru}]^{3+}$ (Fig. 9), as we expect.[20]

In general these polynuclear Os complexes show comparable spectral behaviour to the Ru analogues, with a series of intense NIR transitions whose maximum varies with oxidation state. The assignments however must be different, with LMCT transitions occurring rather than MLCT, reflecting the fact the metals oxidise more easily. Fig. 10 for example illustrates the spectroelectrochemical behaviour of the series $[\mathbf{3\text{-}Os}]^{n+}$ (n = 3–6) in MeCN.

3. Ruthenium and osmium complexes with N- or N,O-donor analogues of dioxolenes

(a) An Os(II)-tris(diimine) complex

As was mentioned above, the N-donor and mixed N,O-donor analogues of the dioxolene series display generally similar ligand-centred redox behaviour as the dioxolenes, albeit with a shift in their redox potentials. The complex $[Os(bqdi)_3]^{2+}$ (bqdi = 1,2-benzoquinone-diimine) was recently prepared by the group of Dr Sreebrata Goswami at the Indian Association for the Cultivation of Science in Calcutta,[21] and its redox and

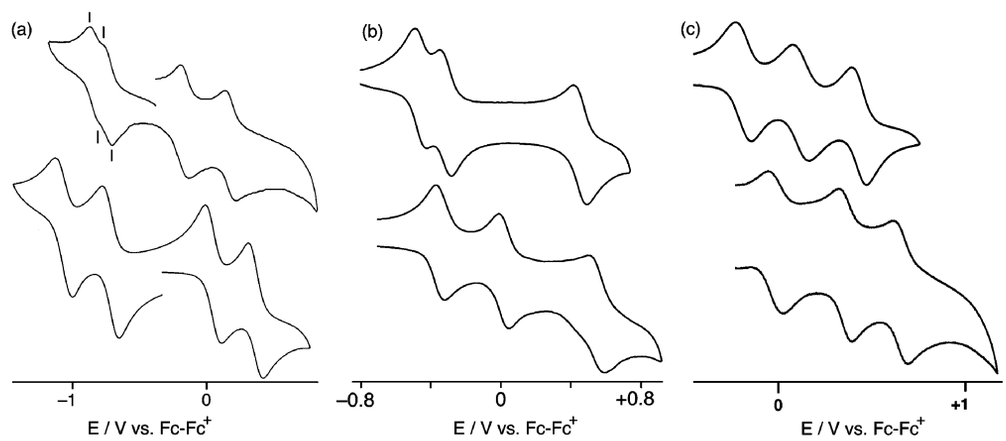

Fig. 9 Comparison of the cyclic voltammograms of (a) $[\mathbf{1\text{-}Os}]^{n+}$ and $[\mathbf{1\text{-}Ru}]^{n+}$; (b) $[\mathbf{3\text{-}Os}]^{n+}$ and $[\mathbf{3\text{-}Ru}]^{n+}$; and (c) $[\mathbf{2\text{-}Os}]^{n+}$ and $[\mathbf{2\text{-}Ru}]^{n+}$. In each case the Os complex is the upper figure and the Ru complex is the lower figure.

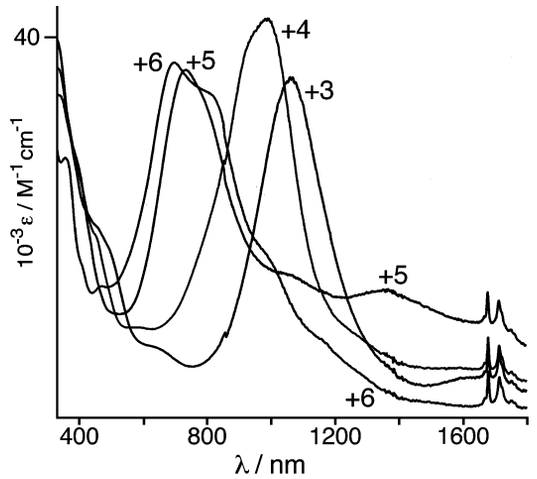

Fig. 10 UV/Vis/NIR spectroelectrochemical study of [**2-Os**]$^{n+}$ (n = 3–6) in MeCN.

spectroscopic properties were studied in Bristol. It is a rare example of an osmium complex with the bqdi redox series; the ruthenium analogue $[Ru(bqdi)_3]^{2+}$ was reported by Warren in 1977.[22] The relatively simple structure of $[Os(bqdi)_3]^{2+}$ (Fig. 11)

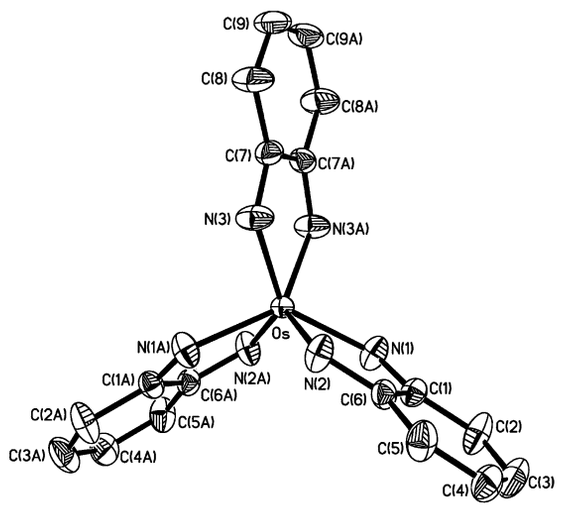

Fig. 11 Crystal structure of the cation of $[Os(bqdi)_3][ClO_4]_2$.

belies the possible ambiguity in its formulation. Like complexes of 1,2-benzoquinone (and, for that matter, the dithiolenes in Scheme 1) it can be assigned a range of formulations ranging from $[Os^{VIII}(opda)]^{2+}$ (where H_2opda = 1,2-diaminobenzene) in which the metal is oxidised and the ligands fully reduced, to $[Os^{II}(bqdi)]^{2+}$ in which the metal is reduced and the ligands fully oxidised. The clearest way to determine the correct oxidation state assignment is crystallographically, because the Os–N distances in the coordination sphere of the metal, and the C–N distances in the ligand, are both diagnostic of the oxidation states of the components involved, and the crystal structure of this complex confirmed its formulation as an Os(II) complex with three neutral bqdi ligands. In particular, (i) the short Os–N distances [average, 1.988(3) Å] are comparable to Os^{II}–N(azo) bond distances (*ca.* 1.98 Å) in complexes where extensive Os–azo π-bonding occurs;[23] and (ii) the C–C and C–N distances in each ligand clearly reflect the alternation of localised single and double bonds around the ring characteristic of a quinonoidal structure.[24]

$[Os(bqdi)_3]^{2+}$ undergoes three chemically reversible one-electron reductions at −0.24, −0.67 and −1.78 V *vs.* Fc/Fc^+ in dmf, for which the obvious assignment is reduction of each ligand in turn to the diimino-benzosemiquinone (dsq) state (*cf.* the q/sq couple in Scheme 1), in agreement with the known ability of diimines to act as effective electron acceptors.[7,15] For comparison, the reductions of $[Ru(bqdi)_3]^{2+}$ occur at 0.03, −0.31 and −1.08 V *vs.* SCE in MeCN.[22] A UV/Vis/NIR study of $[Os^{II}(bqdi)_3]^{2+}$ in all four oxidation states (Fig. 12) confirmed

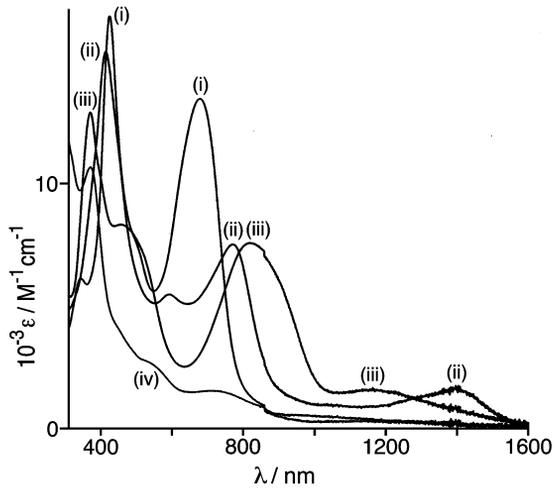

Fig. 12 UV/Vis/NIR spectroelectrochemical study of (i) $[Os(bqdi)_3]^{2+}$, (ii) the singly reduced species $[Os(bqdi)_2(dsq)]^+$, (iii) the doubly reduced species $[Os(bqdi)(dsq)_2]$, and (iv) the monoanionic triply reduced species (see text for formulation) in dmf at 243 K.

this assignment for the first two reductions. Most notably, in the spectra of the mono-reduced species $[Os^{II}(bqdi)_2(dsq)]^+$ and the di-reduced species $[Os^{II}(bqdi)(dsq)_2]$, weak transitions in the NIR region (at 1405 and 1164 nm, respectively) are assignable to inter-valence charge-transfer transitions between reduced and non-reduced ligands, *i.e.* intra-ligand dsq ⟶ bqdi charge transfer transitions. Exactly similar transitions are observed in the reduced forms of $[Ru(bpy)_3]^{2+}$ which contain both unreduced bpy and reduced ($bpy^{\bullet-}$) ligands.[25] However, the spectrum of the triply reduced complex is not obviously consistent with the formulation $[Os^{II}(dsq)_3]^-$, but is more consistent with an internal rearrangement of electrons having occurred to give $[Os^{III}(dsq)_2(opda)]^-$. Such a rearrangement is exactly analogous to the behaviour of the reduced forms of $[Cr(bpy)_3]^{3+}$ described earlier[10–12]—*e.g.* reduction of $[Cr^{II}(bpy)_3]^{2+}$ giving $[Cr^{III}(bpy)(bpy^{\bullet-})]^+$—and is one of the hallmarks of non-innocent behaviour in metal complexes.

(b) A dinuclear Ru(II) complex with a bridging N,O-donor dioxolene analogue

The dinuclear complex [**4-Ru**]$^{2+}$ (Scheme 1) was prepared in the group of Prof. Goutam Lahiri of the Indian Institute of Technology in Bombay, and structural, redox and spectroscopic studies were carried out in Bristol.[26] This complex was the unexpected result of the metal-promoted oxidative coupling of two equivalents of 2-aminophenol. Assignment of the ligand as having this valence structure was assisted by the X-ray crystal structure (Fig. 13): in particular, the short Ru–N separations are characteristic of imine donors (with π back-bonding) but not of amine donors, and in the central 1,4-benzoquinone-diimine (1,4-bqdi) unit the expected alternation of single and double bonds characteristic of a quinonoidal structure is evident. In contrast, the C–C distances in the aromatic ring are quite similar to one another (1.37–1.41 Å).

This bridging ligand may be regarded as comparable to the sq–sq state of complexes [**2Ru**]$^{2+}$ and [**RuN$_4$Ru**]$^{2+}$, in that each chelating bidentate site has one anionic sp^3-hybridised donor atom and one neutral sp^2-hybridised donor atom. This description—of two linked semiquinone units—is clearly not ideal for [**4-Ru**]$^{2+}$, where the bridging 1,4-bqdi unit is in the fully oxidised quinone state with four π-electrons, whereas the other

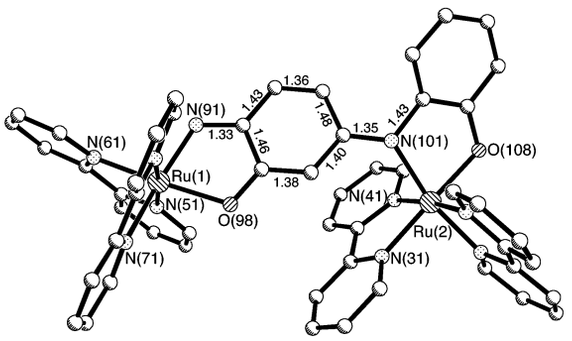

Fig. 13 Crystal structure of the cation of [**4-Ru**][ClO_4]$_2$·2H_2O, showing the bond distances (Å) in the quinonoidal fragment of the bridging ligand.

ring is fully reduced with six π-electrons. Denoting this as a 'sq–sq' state is helpful however in that it emphasises (i) the similarity of the two metal binding sites, and (ii) the relationship of this complex with [**2-Ru**]$^{2+}$ and [**RuN$_4$Ru**]$^{2+}$ (Fig. 5).

Complex [**4-Ru**]$^{2+}$ undergoes several redox processes. There are reversible oxidations at +0.12 and +0.35 V *vs.* SCE, and irreversible oxidations at +1.49 and +1.70 V *vs.* SCE; in addition there are reductions at −0.98, −1.38 and −1.81 V *vs.* SCE which appear reversible on the voltammetric timescale. Of these, it is the central four processes (+0.35, +0.12, −0.98 and −1.38 V) which are the most significant, as they are ligand-centred processes resulting in a five-membered redox chain exactly analogous to those observed for the series [**2**]$^{2+}$ and [**RuN$_4$Ru**]$^{2+}$ (Fig. 5). In fact the three series of complexes have isoelectronic π-systems for a given oxidation state, and the bridging ligand in [**4-Ru**]$^{n+}$ is effectively a positional isomer of those in [**2-Ru**]$^{n+}$ and [**RuN$_4$Ru**]$^{n+}$ but with a mixed donor set. It is significant that the potentials of the redox couples at +0.35 and +0.12 V *vs.* SCE are several hundred mV too negative to be metal-centred on the basis of Lever's electrochemical ligand parameters[27] and by comparison with Ru(II) complexes having similar donor sets;[28] in fact, they lie mid-way between the ligand-centred couples for the O,O-donor and N,N-donor analogues (Fig. 5). We assigned the irreversible oxidations at high potential to Ru(II)/Ru(III) couples, and the couple at −1.81 V to a bpy-centred reduction.

The assignments of the four bridging-ligand centred redox processes were supported by UV/Vis/NIR spectroelectrochemistry (Fig. 14). In [**4-Ru**]$^{2+}$ (sq–sq), the intense transition at 860 nm is a Ru(II) ⟶ (sq–sq) MLCT transition to the LUMO of the bridging ligand, analogous to the transition at 1080 nm for [**1-Ru**]$^{2+}$ (Fig. 4). On oxidation to [**4-Ru**]$^{3+}$ (sq–q state), there are now two closely-spaced MLCT transitions involving the bridging ligand at 892 and 984 nm, since the inherent asymmetry of the ligand means that the valences are localised with distinct 'sq' and 'q' termini. Apart from two distinct MLCT transitions, this also results in an intense, low energy transition at 1570 nm (ε = 9,100 M^{-1} cm^{-1}) which is ascribed to an inter-ligand charge-transfer between the 'semiquinone' and 'quinone' termini of [**4-Ru**]$^{3+}$. Exactly similar behaviour was observed by Lever in [**RuN$_4$Ru**]$^{3+}$ which has localised semiquinone and quinone termini,[15] but such behaviour does not occur in [**2-Ru**]$^{3+}$ where the sq–q state is delocalised.[14] In the fully oxidised state [**4-Ru**]$^{4+}$ (q–q), a typical[5,7] Ru(II) ⟶ diiminoquinone MLCT transition is seen at 607 nm.

The electronic spectra in the reduced oxidation states (Fig. 14) are also consistent with the redox assignments in Fig. 5. On reduction of [**4Ru**]$^{2+}$ to [**4Ru**]$^{+}$(sq–cat), the red-shift of the lowest energy MLCT transition to 1306 nm is exactly consistent with reduction of the bridging 1,4-bqdi unit to give a bridging benzosemiquinone-diimine (1,4-bsqdi) radical, with the new transition being an MLCT transition to the SOMO of the 1,4-bsqdi fragment.[7,15,29] Although this oxidation state is

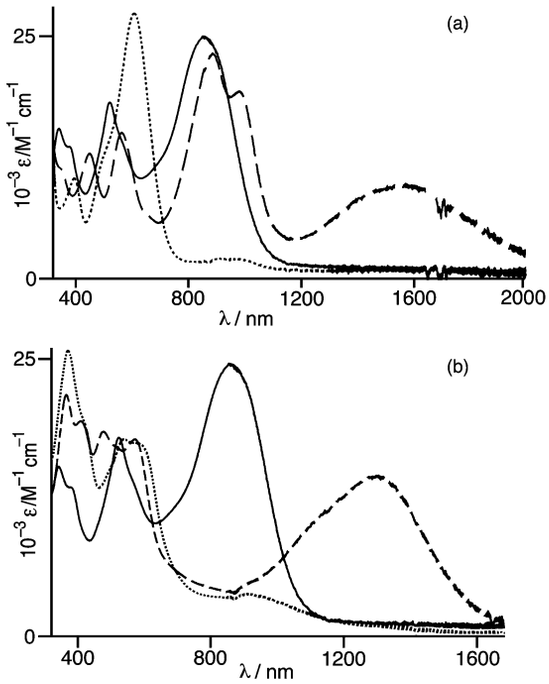

Fig. 14 UV/Vis/NIR spectroelectrochemical study of [**4-Ru**]$^{n+}$ (CH_2Cl_2, 243 K): (a) spectra for n = 2 (—), 3 (---) and 4 (···); (b) spectra for n = 2 (—), 1, (---) and 0 (···).

formally mixed-valence (sq–cat), the fact that the additional electron is localised on the bridging NN unit means that it will be shared equally between the two sites, such that a valence-delocalised description is appropriate (we found no evidence, for example, of an intra-ligand cat ⟶ sq transition associated with localised termini). Further reduction to the fully-reduced state [**4-Ru**] resulted in disappearance of all MLCT transitions, as expected, and appearance of a weak transition at 910 nm which we assign as a (cat–cat)$^{4-}$ ⟶ bpy ligand-to-ligand charge-transfer.[29]

4. Dinuclear ruthenium and molybdenum complexes with non-innocent bridging ligands: effects of non-innocent behaviour on metal–metal electronic coupling

(a) Introduction: electron-transfer and hole-transfer delocalisation through bridging ligands

In the complexes described in the previous sections, the ligands are all derivatives of the basic dithiolene/dioxolene type based on 1,2-disubstituted phenyl rings. In mononuclear complexes (such as [Os(bqdi)$_3$]$^{2+}$),[21] whether the redox processes are metal- or ligand-centred is entirely an internal matter whose electronic consequences do not extend outside the complex. In dinuclear complexes in which there is an electronic interaction between the metal centres however, non-innocent behaviour—the matching of metal and *bridging* ligand redox orbitals—has an additional effect, *viz.* it plays an important rôle in determining the strength of the metal–metal electronic coupling.

This is illustrated by the diagram in Fig. 15, which depicts the frontier orbital arrangement in two hypothetical dinuclear complexes. In the first case, the HOMO of the bridging ligand is close in energy to the metal redox orbital, but the LUMO is very much higher. Oxidation of the metal ion will be similar in energy to oxidation of the bridging ligand, with the result that an oxidised mixed-valence state will be able to delocalise across the bridging ligand: the states M$^+$–L–M and M–L$^+$–M are similar in energy. This amounts to delocalisation by a hole-transfer mechanism.[30] However, reduction of the metal ion is

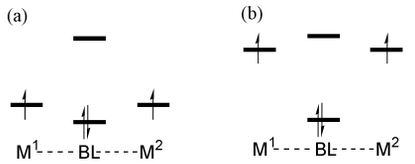

Fig. 15 Simple orbital diagrams showing the situations necessary for delocalisation of metal-based mixed-valence states by (a) hole-transfer through the HOMO of the bridging ligand, and (b) electron-transfer through the LUMO of the bridging ligand.

very different in energy from reduction of the bridging ligand, with the result that a mixed-valence state generated by reduction will not be able to delocalise across the bridging ligand: the state M–L$^-$–M is much higher in energy than M$^-$–L–M. Delocalisation by an electron-transfer mechanism is therefore prevented by the high energy of the bridging ligand LUMO. It is possible in principle that the reduced mixed-valence state M$^-$–L–M could use the accessible HOMO of the bridging ligand for delocalisation by *hole* transfer, which would require formation of the state M$^-$–L$^+$–M$^-$, but this requires charge-separation which is highly endergonic. The second case in Fig. 15 is exactly the converse: the orbitals of the bridging ligand are lower in energy with respect to the metal orbitals, such that the LUMO is close to the metal redox orbitals but the HOMO is remote.[30] A reduced mixed-valence state will be able to delocalise effectively by electron-transfer through the bridging ligand LUMO (M$^-$–L–M ⟶ M–L$^-$–M ⟶ M–L–M$^-$), but hole-transfer is not accessible for delocalisation of an oxidised mixed-valence state (M$^+$–L–M cannot convert to M–L$^+$–M which is a much higher-energy state).

It will be apparent from these simple illustrations that for effective delocalisation of a mixed-valence state the complex needs to show non-innocent behaviour. A mixed-valence state generated by oxidation of one metal will be best delocalised across a bridging ligand which is also oxidisable at a comparable potential. Conversely, a mixed-valence state generated by reduction of one metal requires a reducible bridging ligand for effective delocalisation. If the metal and bridging-ligand redox orbitals are closely matched in energy—*i.e.* highly non-innocent behaviour—then the mixed valence state will be substantially delocalised between both metals, *i.e.* a class III state according to the Robin and Day classification. The availability of electron-transfer and/or hole-transfer pathways for delocalisation in mixed-valence complexes is well known,[30] but it is helpful to consider this in terms of non-innocent behaviour, as the following sections will attempt to demonstrate.

(b) Electron-transfer *vs.* hole-transfer in a pair of mixed-valence Ru(II)/Ru(III) complexes

Designing a pair of complexes to illustrate the above principle requires a pair of complexes with identical termini but different bridging pathways. These requirements at first appear to be mutually exclusive, because changing the bridging ligand means changing at least one of the donor atoms around each metal ion. However this need not result in any change in the co-ordination environment of each metal terminus if there is a compensating change elsewhere in the coordination sphere, and accordingly we prepared the two dinuclear Ru(II) complexes [**5a**]$^{2+}$ and [**5b**]$^{2+}$ (Scheme 2). In each case, both metal centres are in a (pyridyl)$_5$(phenolate) coordination environment, but in complex [**5a**]$^{2+}$ there is a 4,4′-bipyridyl bridge whereas in [**5b**]$^{2+}$ there is a 4,4′-bis(phenolate) bridge.[31]

Complex [**5a**]$^{2+}$ undergoes simultaneous oxidation of both Ru(II) centres to Ru(III) at +0.08 V *vs.* Fc/Fc$^+$. No separation of the two redox processes could be seen, indicative of a weak electronic interaction, consistent with the picture in Fig. 15 above: the oxidised mixed-valence Ru(II)/Ru(III) state cannot delocalise easily across the bipyridyl bridging ligand as the necessary hole-transfer process is difficult. In contrast, complex

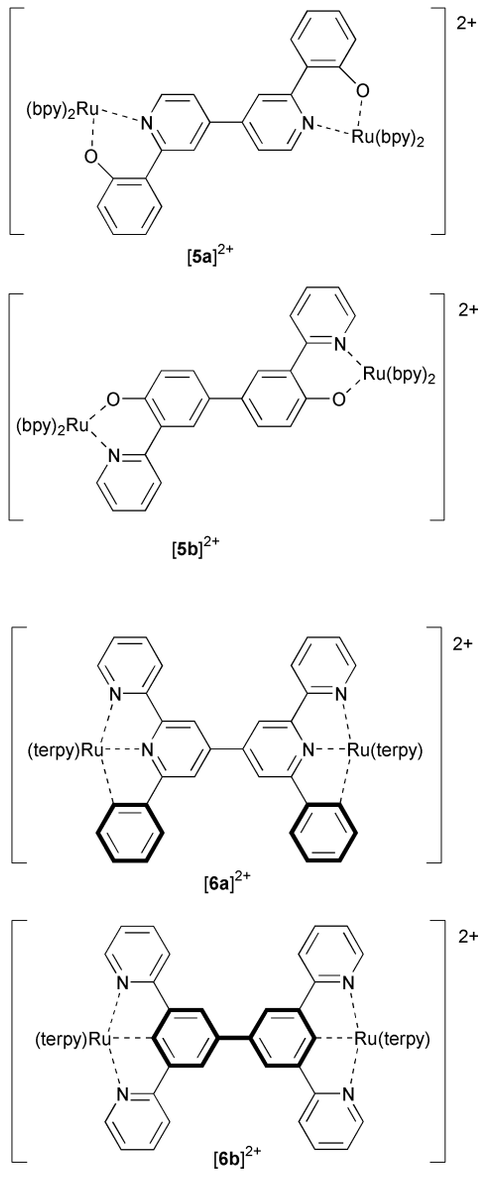

Scheme 2

[**5b**]$^{2+}$ shows two distinct reversible one-electron processes at −0.09 and +0.06 V *vs.* Fc/Fc$^+$, whose separation of 150 mV corresponds to $K_c \approx 350$ for the mixed-valence state [**5b**]$^{3+}$, which can be stabilised by hole-transfer through the (oxidisable) bis-phenolate bridge. In fact two additional irreversible oxidations at more positive potential (+0.76 and +1.02 V *vs.* Fc/Fc$^+$) are assigned to oxidation of the central 4,4′-biphenolate unit to give a quinone;[32] the fact that these processes do not occur in the isomeric complex [**5a**]$^{2+}$ confirms the assignment.

UV/Vis/NIR spectroelectrochemistry (Fig. 16) shows that there is no detectable IVCT transition for [**5a**]$^{3+}$. Although it is not possible to generate the mixed-valence Ru(II)/Ru(III) state [**5a**]$^{3+}$ free from the isovalent states [**5a**]$^{2+}$ and [**5a**]$^{4+}$ because the two redox potentials are so close together, slow increase of the applied potential through the oxidation potential of the complex resulted in a series of spectra showing no evidence at any point for an IVCT transition. If the electronic coupling is weak, any IVCT transition is expected to be of high energy and low intensity (*i.e.* obscured by other transitions). In contrast, the spectrum of [**5b**]$^{3+}$ shows a very obvious IVCT transition centred at 2000 nm (ε = 14,000 M^{-1} cm^{-1}), from whose properties the electronic coupling between the metals can be estimated as 830 cm^{-1}. Despite the greater metal–metal distance, the bis-phenolate bridge of [**5b**]$^{3+}$ affords a stronger metal–metal coupling than the bipyridyl bridge of [**5a**]$^{3+}$

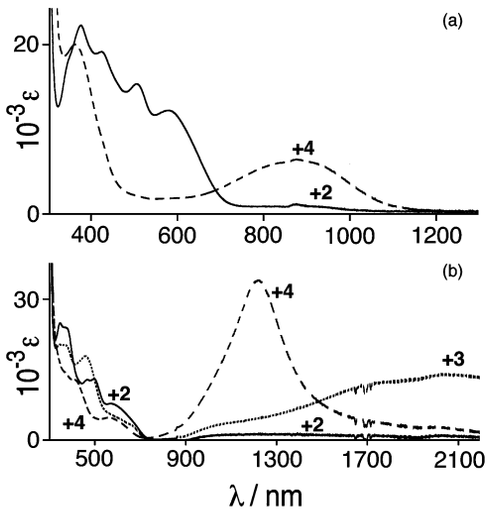

Fig. 16 UV/Vis/NIR spectroelectrochemical study of (a) $[\mathbf{5a}]^{n+}$ (n = 2–4) and (b) $[\mathbf{5b}]^{n+}$ (n = 2–4) (CH_2Cl_2, 243 K).

because of the better matching of the appropriate metal and ligand redox orbitals, *i.e.* non-innocent behaviour.[31]

Similar behaviour was observed by Collin, Launay *et al.* in the isomeric pair of dinuclear complexes $[\mathbf{6a}]^{2+}$ and $[\mathbf{6b}]^{2+}$ (Scheme 2) for an exactly similar reason.[33] In the mixed-valence Ru(II)/Ru(III) forms of the complexes, generated by oxidation, the electronic interaction in $[\mathbf{6b}]^{3+}$ is stronger than that in $[\mathbf{6a}]^{2+}$ because a dianionic biphenyl-diyl bridge can support delocalisation by hole-transfer more effectively than can a neutral bipyridyl bridge. It is interesting to note that many of the early studies on mixed-valency in Ru(II)/Ru(III) complexes used bridging ligands based on pyridyl donors which (with the clear vision of hindsight) are poorly designed from the point of view of optimising electronic interactions in mixed-valence states generated by oxidation![34]

(c) Electron transfer *vs.* hole transfer in mixed-valence dinuclear tris(pyrazolyl)borate-molybdenum complexes

In addition to the work with Ru(II) and Os(II) complexes described above, we have a long-standing interest in the study of polynuclear complexes in which two or more tris(pyrazolyl)-borato-molybdenum fragments are connected by a single bridging ligand, and the electrochemical properties of these provide further insights into the rôle of non-innocent behaviour in determining metal–metal electronic interactions.

The two types of mononuclear complex fragment used for this work are shown in Scheme 3. These are [Mo($Tp^{Me,Me}$)-(NO)Cl(py)] (**7**, where py = pyridine) and [Mo($Tp^{Me,Me}$)(O)-Cl(OPh)] (**8**).[35] Superficially these appear to be electronically quite different, in that **7** is formally a Mo(I) complex, whereas **8** is a Mo(V) complex. However, Enemark has shown that the large difference in oxidation state between these two complexes is more formal than real, because the strongly π-accepting NO ligand in **7** will remove electron-density from the Mo(I) centre whereas the strongly π-donating oxo ligand in **8** will add electron density to the Mo(V) centre.[36] The two complexes show similar redox behaviour, each undergoing a reversible one-electron reduction and a reversible one-electron oxidation. Thus, **7** is part of a Mo(0)/Mo(I)/Mo(II) redox chain, and **8** is part of a Mo(IV)/Mo(V)/Mo(VI) redox chain.[35] In the mononuclear complexes the question of ligand participation in these redox processes does not arise and the redox processes may be regarded as metal-centred in each case.

Use of bis-pyridyl bridging ligands py–X–py (where X is some connecting group linking the pyridyl termini) allows a wide variety of dinuclear Mo^{I}(py–X–py)Mo^{I} complexes to be prepared.[35] Similarly, dinuclear $Mo^{V}(OC_6H_4–X–C_6H_4O)Mo^{V}$

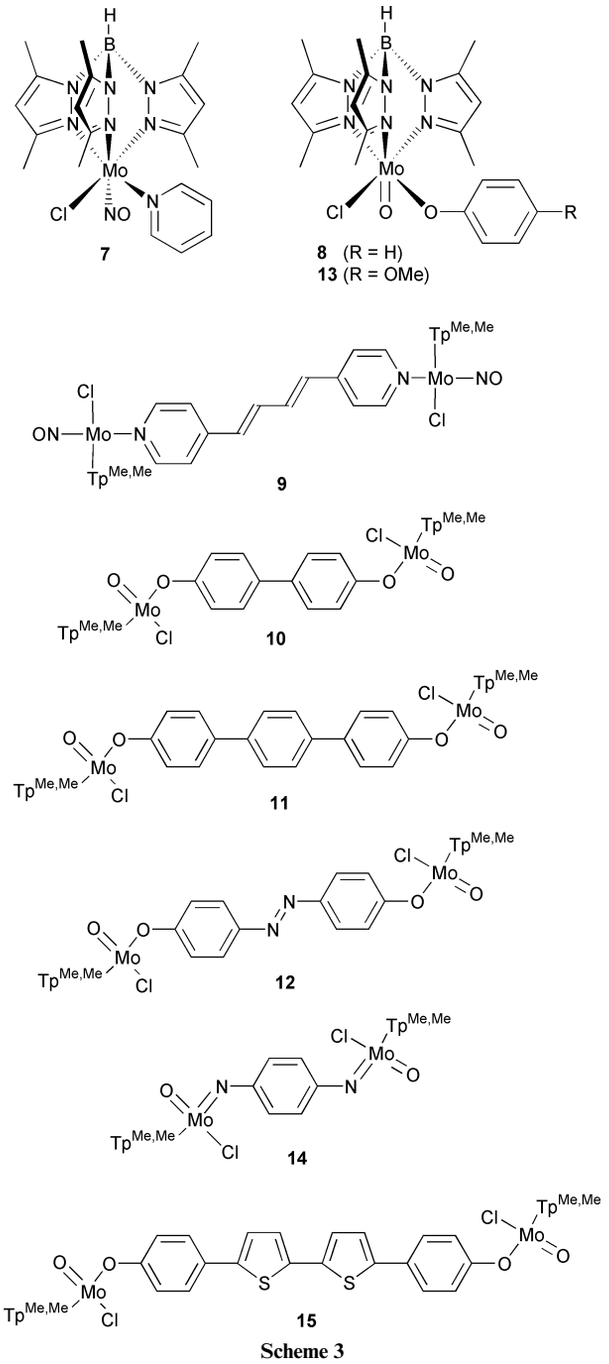

Scheme 3

complexes can be prepared with a wide range of bridging bis-*p*-phenolates;[35] a representative crystal structure of each type is in Fig. 17. Given the redox behaviour of the monomer units **7** and **8**, we expect that the dinuclear complexes will show four redox processes, *viz.* two oxidations and two reductions starting from the neutral complexes. In each case, the separation between an adjacent pair of processes [say, two successive Mo(V)/Mo(VI) couples] will provide a measure of the electronic communication across the bridging ligand. The significance of these complexes is that in one complex we can compare how well *two different* mixed valence states (one generated by oxidation, and one by reduction) are delocalised across the *same* bridging ligand. This is in contrast to the behaviour of complexes $[\mathbf{5a}]^{2+}$ and $[\mathbf{5b}]^{2+}$, in which the behaviour of the *same* mixed-valence state [*i.e.* Ru(II)/Ru(III)] was compared with two different bridging ligands.[31]

Fig. 18 shows the cyclic voltammograms of the complexes [{$Mo^{I}(Tp^{Me,Me})$(NO)Cl}$_2$(μ-py–CH=CH–CH=CH-py)] (**9**)[37] and [{$Mo^{V}(Tp^{Me,Me})$(O)Cl}$_2$(μ-4,4′-biphenolate)][38] (**10**)

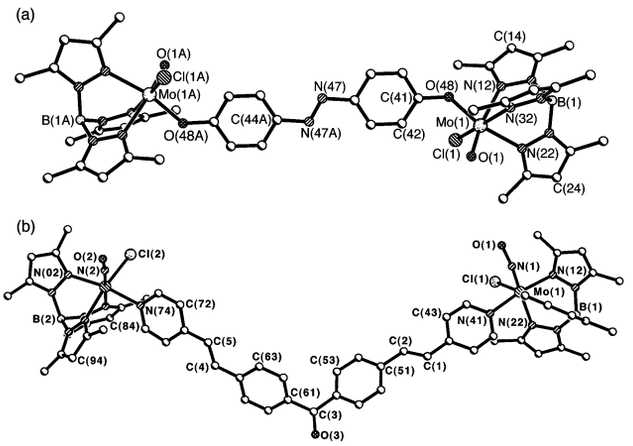

Fig. 17 Crystal structures of typical dinuclear tris(pyrazolyl)borato-molybdenum complexes with extended bridgiing ligands: (a) an oxo-Mo(v) complex with $[OC_6H_4N{=}NC_6H_4O]^{2-}$ as the bridging ligand; (b) a nitrosyl-Mo(I) complex with $NC_5H_4{-}C{\equiv}C{-}C_6H_4{-}C(O){-}C_6H_4{-}C{\equiv}C{-}C_5H_4N$ as the bridging ligand.

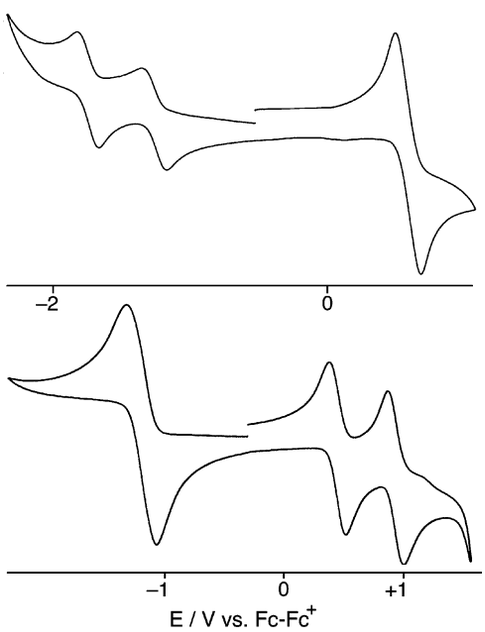

Fig. 18 Cyclic voltammograms of (a) complex **9**, and (b) complex **10**, both in CH_2Cl_2.

(Scheme 3); it will be immediately apparent that (i) they show fundamentally different behaviour, and (ii) this behaviour is consistent with the electron-transfer *vs.* hole-transfer arguments for delocalisation in the mixed-valence states summarised above. For **9**, the two Mo(I)/Mo(0) couples—which are reductions with respect to the neutral starting complex—are separated by 390 mV, whereas the two Mo(I)/Mo(II) oxidations are coincident giving a single double-intensity wave.[37] It follows that the anionic Mo(I)/Mo(0) mixed-valence state of $[\mathbf{9}]^-$ is effectively delocalised through the low-energy LUMO of the bridging ligand, which can act as an effective conduit for electron transfer, *i.e.* $[Mo^0{-}L{-}Mo^I]^- \longrightarrow [Mo^I{-}(L^{\bullet -}){-}Mo^I]^- \longrightarrow [Mo^I{-}L{-}Mo^0]$. In contrast, the HOMO of bipyridyl-type ligands is too high in energy for delocalisation by hole-transfer and the interaction between the two Mo(I)/Mo(II) couples is negligible in comparison. The shorter bridging ligand 4,4′-bpy results in a redox separation of 765 mV between the two Mo(0)/Mo(I) couples in $[\{Mo^I(Tp^{Me,Me})(NO)Cl\}_2(\mu\text{-bpy})]$ ($K_c \approx 10^{13}$ for the mixed-valence state in CH_2Cl_2), which may be compared with the much weaker interaction between the two Ru(II)/Ru(III) oxidations across the same bridging ligand in $[(H_3N)_5Ru{-}(\mu\text{-}4,4'\text{-bpy}){-}Ru(NH_3)_5]^{5+}$ ($K_c = 24$), because of the above-mentioned mismatch between metal and bridging ligand orbitals in the latter case.[39]

In exact contrast to this, the two Mo(v)/Mo(VI) oxidations of **10** are separated by 480 mV ($K_c \approx 10^8$ for the mixed-valence state in CH_2Cl_2) because the HOMO of the oxidisable bis-phenolate bridging ligand is close in energy to the metal d(*xy*) redox orbitals, and can be an effective conduit for delocalisation by hole-transfer; however the LUMO is too high in energy to delocalise the reduced Mo(v)/Mo(IV) mixed-valence state of $[\mathbf{10}]^-$ by electron-transfer and the two Mo(v)/Mo(IV) couples are essentially coincident.[38] Both of these examples, like the pairs of complexes $[\mathbf{5a}]^{2+}/[\mathbf{5b}]^{2+}$ and $[\mathbf{6a}]^{2+}/[\mathbf{6b}]^{2+}$ above, illustrate the importance of non-innocent behaviour in allowing a strong metal–metal interaction in bridged dinuclear complexes.

Very many dinuclear complexes similar to **9** and **10** have been prepared with a variety of bis-pyridyl[35,40] or bis-phenolate[35,41,42] bridging ligands. All show the same general behaviour illustrated by **9** and **10**, with the magnitudes of the redox separations dependent on the exact nature of the additional spacers in the bridging ligand.

(d) Spectroelectrochemical studies on dinuclear tris(pyrazolyl)-borate-molybdenum complexes; evidence for non-innocence

UV/Vis/NIR spectroelectrochemical studies have helped to show that non-innocent behaviour is occurring in complexes of types **9** and **10**. For **9** itself, and its relatives based on extended bis(pyridyl)polyene ligands of the type $NC_5H_4{-}(CH{=}CH)_n{-}C_5H_4N$ (*n* up to 5), one-electron reduction to the "Mo(I)/Mo(0)" state resulted in appearance of intense, low-energy electronic transitions in the NIR region whose fine structure is reminiscent of that shown by polyene radicals.[43] Even if the reduction is largely metal centred (in which case the intense NIR transitions have MLCT character, with charge-transfer from the electron-rich Mo(0) centre to the π* orbital of the bridging bipyridine) the presence of this fine-structure suggests that the reduced forms have some ligand-centred character. Unfortunately the doubly-reduced forms were not stable on the timescale of the spectroelectrochemistry experiment.

More clear-cut evidence for non-innocent behaviour was provided by spectroelectrochemical studies on a range of dinuclear oxo-Mo(v) complexes with bis-phenolate bridging ligands, similar to **10**. For the purposes of illustration we describe the properties of the complexes **11** and **12**, which contain respectively phenylene and an azo spacer groups between the terminal phenolate donors (Scheme 3).[41,42] Starting with the mononuclear model complex $[Mo^V(Tp^{Me,Me})(O)Cl(OC_6H_4\text{-}OMe)]$ (**13**), oxidation to Mo(VI) results in the evolution of electronic spectra shown in Fig. 19(a).[41] The principal change is that the lowest-energy transition, which has phenolate ⟶ Mo(v) LMCT character, is replaced by two phenolate ⟶ Mo(VI) LMCT transitions [there are two because the accepting d(π) orbital set is split by the low-symmetry ligand field]. The lower energy of these is red-shifted compared to the phenolate ⟶ Mo(v) LMCT transition, in agreement with the metal orbitals being lowered in energy on oxidation, and is much more intense. Simplistically, this intense, low-energy phenolate ⟶ Mo(VI) LMCT transition is diagnostic of metal-centred oxidation.

For complex **11**, based on a dihydroxyterphenyl bridge, electronic spectra in the starting Mo(v)/Mo(v) state and the singly and doubly oxidised states are shown in Fig. 19(b).[41] The spectrum of $[\mathbf{11}]^+$ is dominated by an intense, low-energy transition at 1131 nm which we ascribe as phenolate ⟶ Mo(VI) LMCT, *cf.* the behaviour of $[\mathbf{8}]^+$. The dianionic bridging ligand in **11** has a higher-energy HOMO than does monoanionic phenolate, which explains the low energy of the LMCT process. Further oxidation of $[\mathbf{11}]^+$ results in a small change in position (to 1015 nm) but an approximate doubling in intensity of this transition, consistent with the presence of two phenolate ⟶

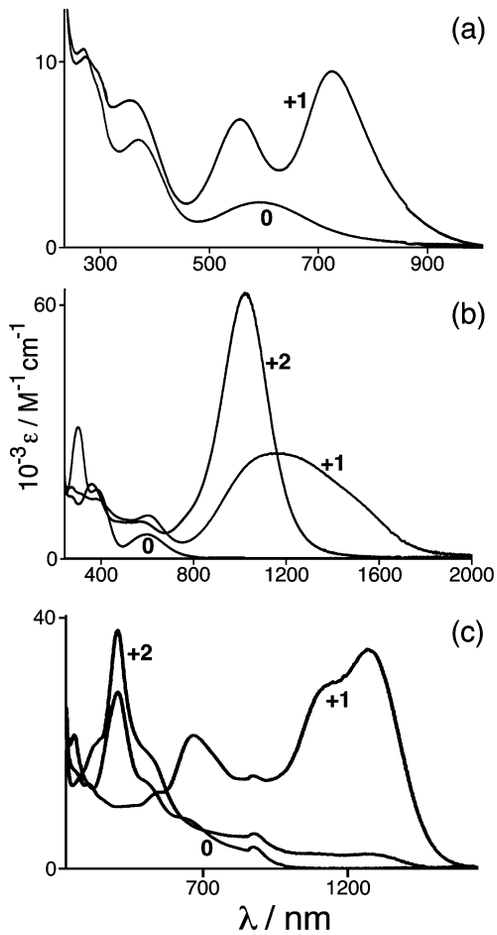

Fig. 19 UV/Vis/NIR spectroelectrochemical studies of (a) $[\mathbf{13}]^{n+}$ ($n = 0$, 1), (b) $[\mathbf{11}]^{n+}$ ($n = 0$–2) and (c) $[\mathbf{12}]^{n+}$ ($n = 0$–2) (CH_2Cl_2, 243 K).

Mo(VI) LMCT processes following successive oxidation of the two metal centres. ZINDO molecular orbital calculations on $[\mathbf{11}]^{2+}$ confirmed this assignment.

Complex **12** contains instead an azo linkage in the bridging ligand between the two phenolate termini, making the bridging ligand planar.[42] The electronic spectra of **12**, $[\mathbf{12}]^{+}$ and $[\mathbf{12}]^{2+}$ are shown in Fig. 19(c) and it is apparent that this complex is behaving quite differently from **11** on oxidation. The first oxidation to $[\mathbf{12}]^{+}$ is, on the basis of the electronic spectrum, metal-centred, with a characteristic low-energy phenolate ⟶ Mo(VI) LMCT transition at 1268 nm. However the second oxidation to $[\mathbf{12}]^{2+}$ results in a substantial change in the spectrum: there is no phenolate ⟶ Mo(VI) LMCT transition, but instead an intense transition at 409 nm in the UV region which is characteristic of a quinone: *i.e.* $[\mathbf{12}]^{2+}$ is best described as Mo^{V}(μ-quinone)-Mo^{V}, in contrast to $[\mathbf{11}]^{2+}$ which is best described as Mo^{VI}(μ-diolate)Mo^{VI}. [It is worth drawing a parallel at this point with the behaviour of complex **14** (Scheme 3), which contains two imido-Mo(VI) units linked by a bridging ligand derived from 1,4-diaminobenzene.[44] This complex undergoes two reversible one-electron oxidations separated by 100 mV which, given the +6 oxidation state of the metals, must be ligand-based resulting in formation of a quinonoidal bridge (Fig. 20). The evolution of electronic spectra during oxidation of **14** to the mono and dications (Fig. 20) is strikingly similar to that which occurs on oxidation of 1,4-diaminobenzene to 1,4-benzoquinone-diimine, confirming the ligand-centred character of these two oxidations to give a bridging quinonoidal unit].[44]

In complex **12**, the change in character from the first oxidation to the second—*i.e.* the first oxidation is metal-centred, but the second oxidation results in an internal rearrangement of electrons such that *both* oxidations are now ligand-centred—is indicative of non-innocent behaviour, as exemplified by the

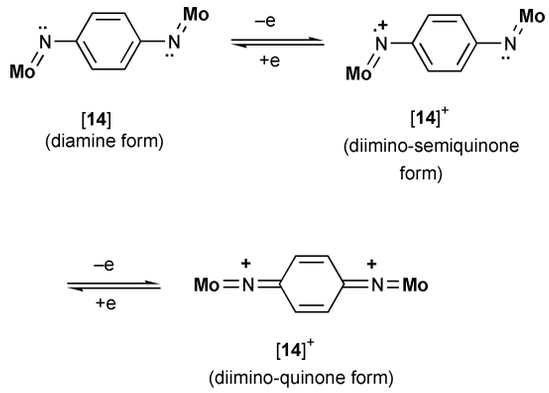

Fig. 20 Ligand-centred oxidations of the bis-imido complex **14** to give a bridging diimino-quinone unit.

sequence of reductions of $[Cr(bpy)_3]^{3+}$ described in Section 1.[11,12] In particular, similar behaviour is shown by complexes of the *o*-dioxolene ligands. Reversible one-electron reduction of $[Ni^{II}(sq)_2]$ affords $[Ni^{III}(cat)_2]^{-}$,[45] in which both ligands become reduced but the metal is oxidised, and identical behaviour is shown by the $[Mn^{II}(sq)_2]/[Mn^{III}(cat)_2]^{-}$ couple.[46] A more dramatic charge redistribution occurs in $[V^{III}(sq)_3]$, which on one-electron reduction affords $[V^{V}(cat)_3]^{-}$; a one-electron reduction of one sq ligand is accompanied by two-electron oxidation of the metal and one-electron reduction of each of the two remaining sq ligands.[47] It appears on the basis of the electronic spectra that complex **12** (amongst others) is behaving in the same way, and that this non-innocence is the principal source of the substantial delocalisation in the Mo(V)/Mo(VI) mixed-valence forms of these complexes [Section 4(c), above].[41,42]

5. Exploitation of the NIR electrochromism: a variable optical attenuator

As mentioned earlier, a characteristic feature of many of these complexes is the presence of intense transitions in the technologically important NIR region of the spectrum, and accordingly we have started to exploit the electrochromism of some of our complexes. Complex **15** (Scheme 3) is another member of the group of dinuclear oxo-Mo(V) complexes also represented by **11** and **12**. In the neutral Mo(V)/Mo(V) state it is transparent in the NIR region, but on one-electron oxidation to the Mo(V)/Mo(VI) state $[\mathbf{15}]^{+}$ develops a particularly low-energy phenolate ⟶ Mo(VI) LMCT transition at 1340 nm ($\varepsilon = 23\,000\ M^{-1}\ cm^{-1}$). A NIR optical switch may be envisaged that operates by rapid and reversible switching between **15** and $[\mathbf{15}]^{+}$.[48]

Complex **12** was incorporated into a two-electrode optically-transparent thin-layer electrode (OTTLE) cell based on two conducting glass slides. The absorption of the cell containing an acetonitrile solution of **15** was monitored at a wavelength of 1160 nm while a stepped potential was applied to the electrodes alternating above and below the first oxidation potential of **15**. Repeated stepping of the applied potential between 0 and 1.5 V showed reversible optical switching; Fig. 21(a) illustrates the change in absorption with the applied voltage, a process which was repeatable over several thousand cycles.

We then evaluated the material as a *variable optical attenuator*, *i.e.* as a mechanism for providing a controlled degree of attenuation of a 1300 nm laser—effectively, a NIR dimmer switch. The variable optical attenuator is a key component in advanced wavelength division multiplexed networks and, ideally, requires a high degree of attenuation (for this complex, a high optical density) at low cost (*i.e.* modest applied potential). Using an acetonitrile solution of **15** in a cell with a 6 mm optical path length and a 1300 nm Fabry–Perot laser as a

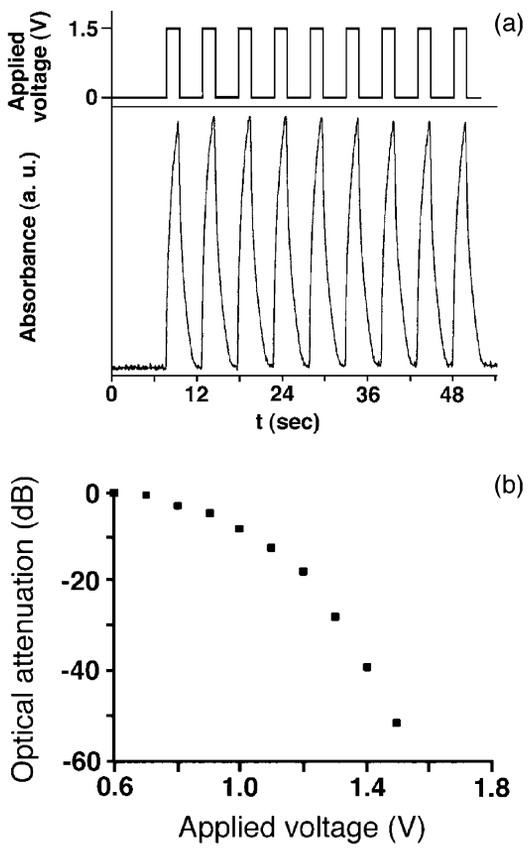

Fig. 21 Near-infrared optical switching using the **[15]**/**[15]**$^{+}$ couple: (a) reversible optical absorption of **15**/**[15]**$^{+}$ at $\lambda = 1160$ nm with an applied voltage cycled between 0 (3 s) and +1.5 V (2 s); (b) variable attenuation of a 1300 nm laser as a function of applied potential using a solution of **15** in MeCN.

light source, the variation in optical power out of the sample for differing applied voltages was measured [Fig. 21(b)]; the attenuation reaches a maximum of 50 dB at an applied potential of 1.5V.[48] This degree of attenuation (99.999%) at a relatively low voltage is comparable to the best that is currently available from alternative attenuator technologies.[49] At the moment the switching process in solution is very slow, and current efforts are directed at anchoring molecules such as **15** to surfaces to increase the switching rates.

6. Conclusions and future directions

This review has described a wide range of complexes in which spectroelectrochemical studies have been used as an informative handle to help understand non-innocent redox behaviour. In particular we have made the point that non-innocence is not confined to complexes of chelating ligands such as dioxolenes and dithiolenes, but also occurs in *bridging* ligands, where non-innocent behaviour has a profound effect on metal–metal electronic interactions and the properties of mixed-valence complexes. As a spin-off from this work, the intense, low-energy (NIR) electronic transitions that are a feature of such complexes are starting to be exploited in optical materials-related applications.

Acknowledgements

We extend our thanks to all of the undergraduate, graduate and post-doctoral research workers who have been responsible for producing these results: their names appear in the reference list below. We also thank our various collaborators: Dr Sreebrata Goswami and Prof. Goutam Lahiri for providing complexes $[Os(bqdi)_3][ClO_4]_2$ and **[4-Ru]**$[ClO_4]_2$ respectively for spectroelectrochemical analysis; and Profs. Ian White and Richard Penty of the Engineering department in Bristol for measurements of the 'variable optical attenuator' described in Section 5. We are especially grateful to Prof. Karl Wieghardt for some excellent lectures and helpful discussions on non-innocent behaviour which helped us to make sense of our results. Finally, we thank the EPSRC for much of the funding which has supported this research.

References

1 G. N. Schrauzer and V. Mayweg, *J. Am. Chem. Soc.*, 1962, **84**, 3221; A. Davison, N. Edelstein, R. H. Holm and A. H. Maki, *J. Am. Chem. Soc.*, 1963, **85**, 2029; A. Davison, N. Edelstein, R. H. Holm and A. H. Maki, *Inorg. Chem.*, 1963, **2**, 1227; H. B. Gray, R. Williams, I. Bernal and E. Billig, *J. Am. Chem. Soc.*, 1962, **84**, 3596; E. Billig, R. Williams, I. Bernal, J. H. Waters and H. B. Gray, *Inorg. Chem.*, 1964, **3**, 663; J. A. McCleverty, *Prog. Inorg. Chem.*, 1968, **10**, 49.
2 C. G. Pierpont and C. W. Lange, *Prog. Inorg. Chem.*, 1994, **41**, 331; C. G. Pierpont, *Coord. Chem. Rev.*, 2001, **216**, 99.
3 O.-S. Jung, D. H. Jo, Y.-A. Lee, B. J. Conklin and C. G. Pierpont, *Inorg. Chem.*, 1997, **36**, 19.
4 R. S. da Silva, S. I. Gorelsky, E. S. Dodsworth, E. Tfouni and A. B. P. Lever, *J. Chem. Soc., Dalton Trans.*, 2000, 4078; A. B. P. Lever, H. Masui, R. A. Metcalfe, D. J. Stufkens, E. S. Dodsworth and P. R. Auburn, *Coord. Chem. Rev.*, 1993, **125**, 317; P. R. Auburn, E. S. Dodsworth, M. Haga, W. Liu, W. A. Nevin and A. B. P. Lever, *Inorg. Chem.*, 1991, **30**, 3502.
5 M. Haga, E. S. Dodsworth and A. B. P. Lever, *Inorg. Chem.*, 1986, **25**, 447.
6 A. B. P. Lever and S. I. Gorelsky, *Coord. Chem. Rev.*, 2000, **208**, 153; C. J. da Cunha, E. S. Dodsworth, M. A. Monteiro and A. B. P. Lever, *Inorg. Chem.*, 1999, **38**, 5399; M. Ebadi and A. B. P. Lever, *Inorg. Chem.*, 1999, **38**, 467; S. I. Gorelsky, E. S. Dodsworth, A. B. P. Lever and A. A. Vlcek, *Coord. Chem. Rev.*, 1998, **174**, 469; R. A. Metcalfe and A. B. P. Lever, *Inorg. Chem.*, 1997, **36**, 4762.
7 H. Chun, T. Weyhermüller, E. Bill and K. Wieghardt, *Angew. Chem., Int. Ed.*, 2001, **40**, 2489; P. Chaudhuri, C. N. Verani, E. Bill, E. Bothe, T. Weyhermuller and K. Wieghardt, *J. Am. Chem. Soc.*, 2001, **123**, 2213.
8 C. K. Jørgensen, *Coord. Chem. Rev.*, 1966, **1**, 164.
9 A. Juris, V. Balzani, F. Barigeletti, S. Campagna, P. Belser and A. von Zelewsky, *Coord. Chem. Rev.*, 1988, **84**, 85.
10 M. C. Hughes and D. J. Macero, *Inorg. Chem.*, 1976, **15**, 2041.
11 I. Hanazaki and S. Nagakura, *Bull. Chem. Soc. Jpn.*, 1971, **44**, 2312.
12 K. Nakemoto, Y. Saito, J. Takemoto and B. Hutchison, *Inorg. Chem.*, 1972, **11**, 2003; E. Konig and S. Herzog, *J. Inorg. Nucl. Chem.*, 1970, **32**, 585.
13 M. Haga, K. Isobe, S. R. Boone and C. G. Pierpont, *Inorg. Chem.*, 1990, **29**, 3795.
14 L. F. Joulié, E. Schatz, M. D. Ward, F. Weber and L. J. Yellowlees, *J. Chem. Soc., Dalton Trans.*, 1994, 799.
15 P. R. Auburn and A. B. P. Lever, *Inorg. Chem.*, 1990, **29**, 2551.
16 R. J. Mortimer, *Chem. Soc. Rev.*, 1997, 147; R. J. Mortimer, *Electrochim. Acta*, 1999, **44**, 2971; D. Rosseinsky and R. J. Mortimer, *Adv. Mater.*, 2001, **13**, 783; M. Emmelius, G. Pawlowski and H. W. Vollmann, *Angew. Chem., Int. Ed. Engl.*, 1989, **28**, 1445; J. Fabian and R. Zahradnik, *Angew. Chem., Int. Ed. Engl.*, 1989, **28**, 677; J. Fabian, H. Nakazumi and M. Matsuoka, *Chem. Rev.*, 1992, **92**, 1197.
17 M. K. Nazeeruddin, P. Pechy, T. Renouard, S. M. Zakeeruddin, R. Humphry-Baker, P. Comte, P. Liska, L. Cevey, E. Costa, V. Shklover, L. Spiccia, G. B. Deacon, C. A. Bignozzi and M. Grätzel, *J. Am. Chem. Soc.*, 2001, **123**, 1613; M. K. Nazeeruddin, R. Humphry-Baker, M. Grätzel, D. Wohrle, G. Schnurpfeil, G. Schneider, A. Hirth and N. Trombach, *J. Porph. Phthalocyanines*, 1999, **3**, 230.
18 A. M. Barthram, R. L. Cleary, R. Kowallick and M. D. Ward, *Chem. Commun.*, 1998, 2695.
19 A. M. Barthram and M. D. Ward, *New J. Chem.*, 2000, **24**, 501.
20 A. M. Barthram, Z. R. Reeves, J. C. Jeffery and M. D. Ward, *J. Chem. Soc., Dalton Trans.*, 2000, 3162.
21 A. K. Ghosh, S.-M. Peng, R. L. Paul, M. D. Ward and S. Goswami, *J. Chem. Soc., Dalton Trans.*, 2001, 336.
22 L. F. Warren, *Inorg. Chem.*, 1977, **16**, 2814.
23 B. K. Ghosh, A. Mukhopadhyay, S. Goswami, S. Ray and A. Chakravorty, *Inorg. Chem.*, 1984, **23**, 4633.

24 O. Carugo, K. Djinovic, M. Rizzi and C. N. Castellani, *J. Chem. Soc., Dalton Trans.*, 1991, 1551.
25 G. A. Heath, L. J. Yellowlees and P. S. Braterman, *Chem. Phys. Lett.*, 1982, **92**, 646.
26 S. Chakraborty, R. H. Laye, R. L. Paul, V. G. Puranik, M. D. Ward and G. K. Lahiri, *J. Chem. Soc., Dalton Trans.*, in press.
27 S. S. Fielder, M. C. Osborne, A. B. P. Lever and W. J. Pietro, *J. Am. Chem. Soc.*, 1995, **117**, 6990.
28 S. Chakraborty, M. G. Walawalkar and G. K. Lahiri, *J. Chem. Soc., Dalton Trans.*, 2000, 2875; B. M. Holligan, J. C. Jeffery, M. K. Norgett, E. Schatz and M. D. Ward, *J. Chem. Soc., Dalton Trans.*, 1992, 3345; A. M. W. Cargill Thompson, J. C. Jeffery, D. J. Liard and M. D. Ward, *J. Chem. Soc., Dalton Trans.*, 1996, 879.
29 N. C. Fletcher, T. C. Robinson, A. Behrendt, J. C. Jeffery, Z. R. Reeves and M. D. Ward, *J. Chem. Soc., Dalton Trans.*, 1999, 2999.
30 G. Giuffrida and S. Campagna, *Coord. Chem. Rev.*, 1994, **135–136**, 517; C. E. B. Evans, M. L. Naklicki, A. R. Rezvani, C. A. White, V. V. Kondratiev and R. J. Crutchley, *J. Am. Chem. Soc.*, 1998, **120**, 13096.
31 R. H. Laye, S. M. Couchman and M. D. Ward, *Inorg. Chem.*, 2001, **40**, 4089.
32 J. Zhou and A. Rieker, *J. Chem. Soc., Perkin Trans. 2*, 1997, 931.
33 C. Patoux, J.-P. Launay, M. Beley, S. Chodorowski-Kimmes, J.-P. Collin, S. James and J.-P. Sauvage, *J. Am. Chem. Soc.*, 1998, **120**, 3717.
34 M. D. Ward, *Chem. Soc. Rev.*, 1995, 121; D. E. Richardson and H. Taube, *Coord. Chem. Rev.*, 1984, **60**, 107; C. Creutz, *Prog. Inorg. Chem.*, 1983, **30**, 1.
35 J. A. McCleverty and M. D. Ward, *Acc. Chem. Res.*, 1998, **31**, 842.
36 B. L. Westcott and J. H. Enemark, *Inorg. Chem.*, 1997, **36**, 5404.
37 S. L. W. McWhinnie, C. J. Jones, J. A. McCleverty, D. Collison and F. E. Mabbs, *J. Chem. Soc., Chem. Commun.*, 1990, 940.
38 V. A. Ung, D. A. Bardwell, J. C. Jeffery, J. P. Maher, J. A. McCleverty, M. D. Ward and A. Williamson, *Inorg. Chem.*, 1996, **35**, 5290.
39 M. J. Powers and T. J. Meyer, *J. Am. Chem. Soc.*, 1980, **102**, 1289; J. E. Sutton and H. Taube, *Inorg. Chem.*, 1981, **20**, 3125.
40 A. J. Amoroso, A. M. W. Cargill Thompson, J. P. Maher, J. A. McCleverty and M. D. Ward, *Inorg. Chem.*, 1995, **34**, 4828; A. M. W. Cargill Thompson, D. Gatteschi, J. A. McCleverty, J. A. Navas Badiola, E. Rentschler and M. D. Ward, *Inorg. Chem.*, 1996, **35**, 2701; V. A. Ung, A. M. W. Cargill Thompson, D. A. Bardwell, D. Gatteschi, J. C. Jeffery, J. A. McCleverty, F. Totti and M. D. Ward, *Inorg. Chem.*, 1997, **36**, 3447.
41 N. C. Harden, E. R. Humphrey, J. C. Jeffery, S.-M. Lee, M. Marcaccio, J. A. McCleverty, L. H. Rees and M. D. Ward, *J. Chem. Soc., Dalton Trans.*, 1999, 2417.
42 S. R. Bayly, E. R. Humphrey, H. de Chair, C. G. Paredes, Z. R. Bell, J. C. Jeffery, J. A. McCleverty, M. D. Ward, F. Totti, D. Gatteschi, S. Courric and C. G. Screttas, *J. Chem. Soc., Dalton Trans.*, 2001, 1401.
43 S. L. W. McWhinnie, J. A. Thomas, T. A. Hamor, C. J. Jones, J. A. McCleverty, D. Collison, F. E. Mabbs, C. J. Harding, L. J. Yellowlees and M. G. Hutchings, *Inorg. Chem.*, 1996, **35**, 760.
44 S.-M. Lee, R. Kowallick, M. Marcaccio, J. A. McCleverty and M. D. Ward, *J. Chem. Soc., Dalton Trans.*, 1998, 3443.
45 C. W. Lange and C. G. Pierpont, *Inorg. Chim. Acta*, 1997, **263**, 219.
46 S. K. Larsen, C. G. Pierpont, G. De Munno and G. Dolcetti, *Inorg. Chem.*, 1986, **25**, 4828.
47 M. E. Cass, N. R. Gordon and C. G. Pierpont, *Inorg. Chem.*, 1986, **25**, 3962.
48 A. McDonagh, S. R. Bayly, D. J. Riley, M. D. Ward, J. A. McCleverty, M. A. Cowin, C. N. Morgan, R. Varrazza, R. V. Penty and I. H. White, *Chem. Mater.*, 2000, **12**, 2523.
49 B. Barber, C. R. Giles, V. Askyuk, R. Ruel, L. Stulzl and D. Bishop, *IEEE Photonics Technol. Lett.*, 1998, **10**, 1262; T. Kawai, M. Koga, M. Okuno and T. Kitoh, *Electron. Lett.*, 1998, **34**, 264; Y.-S. Jin, S.-S. Lee and Y.-S. Son, *Electron. Lett.*, 1999, **35**, 916.